the wound rotor configuration [12], and doubly fed induction generator (DFIG) wind energy generators [13], [14]. These DTC control methods are computationally simple and are able to eliminate the rotor position sensors. Similar to the induction motor DTC, direct power control (DPC) for synchronous rectifiers has also been explored [15]–[20]. With DPC control, the instantaneous active and reactive powers are directly controlled in a manner analogous to torque and flux control in an induction motor. Some control schemes are associated with sensorless operation where the voltage sensors are removed and the point-of-common-coupling (PCC) voltage is estimated by using the reported algorithm in [15], although the current sensors are still required. However, the application of DPC to active filters has not been considered so far for compensation of high-frequency harmonics [21]. In addition, the PWM gating signals are fed directly from the hysteresis controller in the previous DPC methods; therefore, there is no regulation of the switching frequency in most of the reported works. Fixing the switching frequency of the PWM converter has been discussed in [22]–[24], based on the motor parameters, but was limited to specific motor drive applications.

This paper has applied the instantaneous active and reactive power terms based on [25]–[27], and formulated the appropriate power terms for the DPC of shunt-connected active filters, which are different from those applied in synchronous rectifiers in [28]–[30]. The high-performance switching functions have been derived systematically based on power injection requirements under different compensation conditions. Since the phase information of the PCC voltage needs to be used for the selection of the switching states, this paper has proposed a new algorithm to identify the sectors where the voltage vector is located. The proposed phase tracking algorithm only involves simple algebraic and logical computations, and avoids intensive trigonometric functions as well as consequent approximation errors. This new phase tracking algorithm is oriented to active filter applications; all the required variables are also used in instantaneous power calculation. In addition, the proposed controller dynamically adjusts the bandwidth of the hysteresis comparators and limits the PWM switching frequency to eliminate the unnecessary short switching pulses in extremely noisy cases, and the control system can be used directly and effectively for various types of nonlinear load compensation.

Compared to the commonly used proportional-integral (PI) control structure, the proposed DPC directly uses power terms as control variables, and integrates control and modulation functions. Therefore, the *abc-dq0* coordinates transformation and the dedicated PWM modulator are no longer required in the proposed DPC. Compared to the DPC applications reported in previous works, the proposed method is oriented to compensate high-frequency harmonics caused by nonlinear loads [31]; the switching functions are redefined, the bandwidth of the DPC controllers is dynamically adjusted, and the averaged switching frequency is regulated to optimize the performance.

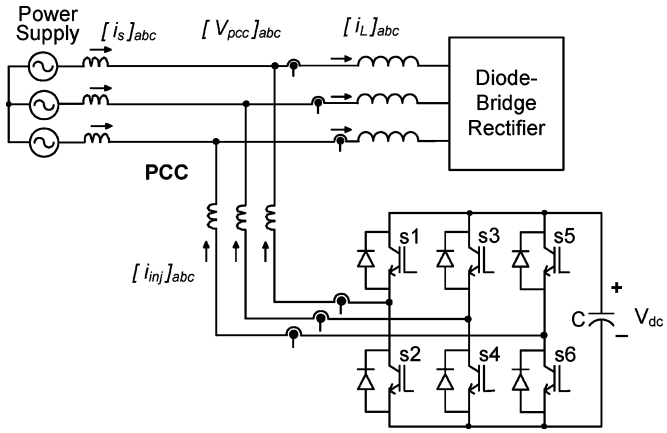

Fig. 1. Power circuit of the shunt-connected active filter.

The proposed DPC controller is tested on a 2-kVA laboratory prototype for load harmonics filtering and load fluctuation compensation. Simulation and experimental results confirm that the proposed DPC control is robust and insensitive to load conditions, and provides good steady state and dynamic performance.

II. Description of the Active Filter System

The proposed shunt-connected active filter uses a standard three-phase two-level voltage source inverter, as shown in Fig. 1.

The proposed DPC method directly uses power quantities as control variables, and the entire control algorithm is carried out in stationary *abc* coordinates. The instantaneous power terms used in this paper are similar to those reported in [1]. The instantaneous active and reactive powers injected by the active filter are expressed in (1), as shown at the bottom of the page.

The instantaneous active power reference $p^*_{\rm inj}$ is generated based on the instantaneous active power ripples drawn by the nonlinear load, plus the power requirement of the dc bus voltage control loop to compensate switching loss. The instantaneous reactive power reference $q^*_{\rm inj}$ is equal to the instantaneous reactive power ripples consumed by the nonlinear load. Using a simplified block diagram, the DPC control reference generation scheme is shown in Fig. 2.

With DPC, two hysteresis comparators are used for control purposes and the corresponding PWM gating signals are generated based on the output of the comparators. The instantaneous power differences (ψ_p, ψ_q) between the active filter injection and those drawn by the nonlinear load are limited within the preselected hysteresis bandwidth. As a result, the active filter compensates for the power ripples drawn by the nonlinear

$$p_{\rm inj} = v_{{\rm pcc},a} i_{{\rm inj},a} + v_{{\rm pcc},b} i_{{\rm inj},b} + v_{{\rm pcc},c} i_{{\rm inj},c}$$
$$q_{\rm inj} = \frac{-(v_{{\rm pcc},a}(i_{{\rm inj},b} - i_{{\rm inj},c}) + v_{{\rm pcc},b}(i_{{\rm inj},c} - i_{{\rm inj},a}) + v_{{\rm pcc},c}(i_{{\rm inj},a} - i_{{\rm inj},b}))}{\sqrt{3}}. \quad (1)$$

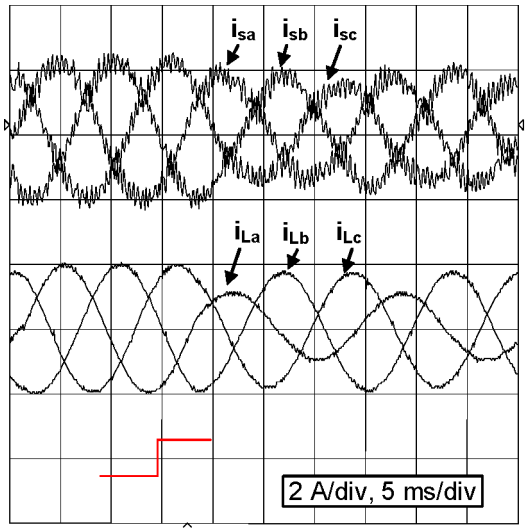

(a)

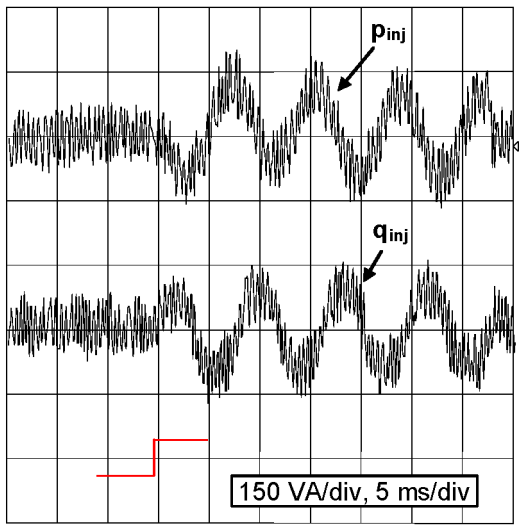

(b)

Fig. 9. Performance of the active filter for unbalanced load compensation. (a) Three-phase supply current (upper) and load current (lower) with load in phase-A reduced to 50%. x-axis: 5 ms/div and y-axis: 2 A/div. (b) Injected instantaneous power p (upper) and q (lower), the ripple is of 120 Hz. x-axis: 5 ms/div and y-axis: 150 VA/div.

Fig. 8. Performance of the active filter for harmonic current filtering. (a) Input current (upper), load current (middle), and injected current (lower) of the active filter. (b) Harmonic spectrum of input current (upper), load current (middle), and injected current (lower). (c) Injected instantaneous power p (upper) and q (lower), the ripple is of 300–420 Hz.

is less than 7 kHz, and as a consequence, the switching frequency increases accordingly. To compensate for this, the bandwidth is tuned to increase when the switching frequency is higher than 8 kHz so as to force the switching frequency to decrease. The change of the PWM switching frequency always follows the regulation of the bandwidth. Results show that the switching frequency is controlled in the range of 5.5–8.5 kHz by using the variable bandwidth between 2–5 var. Fig. 11(b) plots the averaged switching frequency as a function of the comparator bandwidth for harmonic current compensation. A large amount of load harmonics will be injected into the ac system when the bandwidth is larger than 12 var, which should be avoided in implementation.